



Analysis of sound field variations in concert halls via visualization and objective parameter comparison

Sébastien Barré¹, Olaf Jaeckel¹ and Ralf Bauer-Diefenbach²

¹GFaI Gesellschaft zur Förderung angewandter Informatik e.V.

Volmerstraße 3, 12489 Berlin, Germany

²MMT Network GmbH

Helmholtzstraße 2-9, 10587 Berlin, Germany

Abstract

The application of spherical microphone arrays in the field of room acoustics allows for a more detailed analysis of the behaviour of the sound field characteristics and therefore it may be a very valuable supplement of standard room acoustic measurement procedures. With the objective of exemplifying and expanding the application of 3D-beamforming techniques to the field of room and building acoustics, a series of measurements has been performed in real environments. This paper presents the results of an exemplary measurement session performed at the Werner Otto hall of the Konzerthaus Berlin. The measurement results demonstrated the ability of the new microphone array techniques to confirm the differences of the acoustic characteristics of the room before and after application of a special acoustic treatment placed behind and beside the stage.

1 Introduction

THIS paper presents the application of a 3D-microphone array system in the field of room acoustics. The development of correlation and spectral deconvolution methods ([4], [5]) allows the determination of room impulse responses for every individual microphone within the spherical array. Combined with 3D-beamforming techniques to create acoustic surface maps in the room, a detailed analysis of room reflections and of further sound field characteristics is provided. In the following, the application of this method is demonstrated using the results of an exemplary measurement session performed at the Werner Otto hall of the Konzerthaus Berlin. According to the subjective evaluation given by musicians and by the technical directorate of the Konzerthaus Berlin, the acoustic of the Werner Otto hall is considered highly absorptive,

with inevitable corollaries of an unbalance distribution, an insufficient blend of the reverberant sound field which has unfortunate consequences in orchestral music performances, and the seats most distant from the stage are acoustically highly disadvantaged. Additionally, in particular room conditions an audible echo emerges between parallel partitions of the room. The analysis of the microphone array measurement results in combination with classical room acoustic analysis can give a precise description of the acoustic characteristics of the room, and it emphasizes the benefits of placing wooden standing panels behind and beside the stage. The resulting 3D acoustic pictures have been matched to the results of a 3D scan of the interior of the concert hall, the distribution of the acoustic energy in the room has been analyzed, and the results are given and discussed.

2 Measurement setup

The Werner Otto Saal was built in a modern small-size shoe-box shape configuration, with an elevating system which offers the possibility to adjust the height of the stage and of the audience (as depicted by the lower schematics of figure [1]). During the measurement, the stage was set at level 0 and the audience was in a gradually elevated floor arrangement.

One source position (on the stage) and two receiver positions were selected for the measurement (one on the stage and one at the fifth row of seats). The receiver positions will be designated as *Stage* and *Audience* in the following. The source and receiver positions as well as the room configuration are presented figure [1]. Twenty room impulse response measurements were performed using MLS signal as well as sine sweeps. After a first measurement session at both receiver positions, RESPA© standing resonators were placed behind and beside the stage, and new measurements have been performed. The RESPA© resonators are wooden made panels which resonate with the sound field of the room. Their development has been inspired by the technique of the (centuries-old) lutherie craft to enhance the processes of resonance.

One transparent spherical array of 120 microphones together with an Acam Recorder were used, the room was excited using a Globesource dodecahedron and an RME-Babyface Soundcard. The dodecahedron was supported in the low frequency range by a Meyersound Subwoofer. Additionally to the measurement with the Acoustic Camera, a type 1 microphone from G.R.A.S. was used to capture the sound field at the source for the reference signal and a Microtech Gefell type 1 microphone at the receiver position was used for verification.

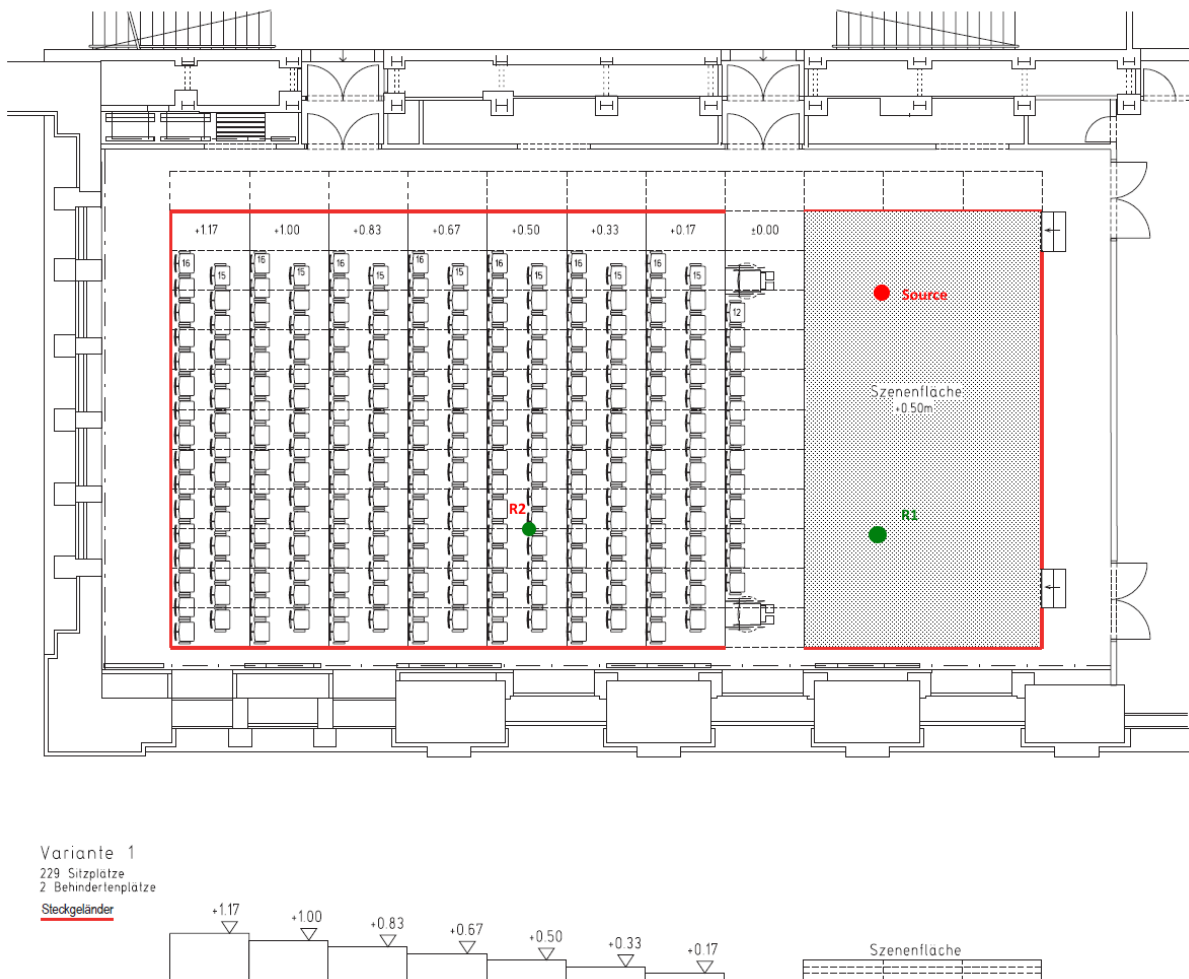


Figure 1: Seating plan of the Werner Otto hall and measurement positions (the receiver positions are indicated by the green marks, the red mark indicates the source position).
 © Konzerthaus Berlin.

3 Impulse response

The impulse responses of each of the 120 signals captured by the microphones of the array were computed. As described in ISO-18233 [1] a linear deconvolution is performed in the frequency domain (equation 1) between the N signals $y_i(t)$ and the original signal $x(t)$ sent to the room. The measurement and processing principle is presented in the schematics [2].

$$h_i(t) = IFFT \left[\frac{FFT(y_i(t))}{FFT(x(t))} \right] \quad (1)$$

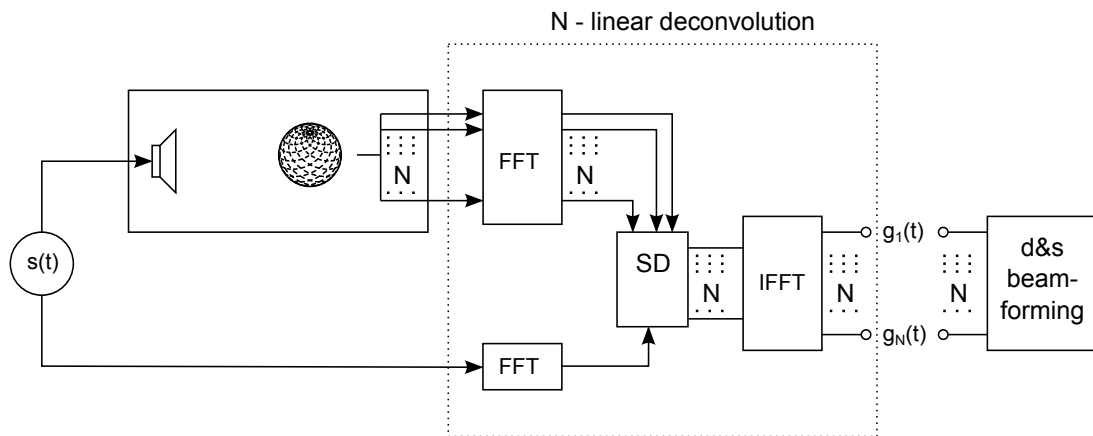


Figure 2: Measurement principle: the loudspeaker excites the room with a sine-sweep signal that propagates and reaches the N microphones of the array. The linear deconvolution stage is performed via regularized spectral division (SD) of the Fourier transform (FFT) of the N signals coming from the array by the Fourier transform of the original signal sent to the room. After an inverse-FT (IFFT), the resulting impulse responses are processed by delay-and-sum (d&s) beamforming.

The linearity of the deconvolution process preserves the relative delay of arrival between each signal of each microphone ([4], [5]) and therefore, by sending the result of the deconvolution process directly to the beamformer, it is possible to localize the source, as well as the hits of the acoustic waves that arrive at the array on the walls of the room.

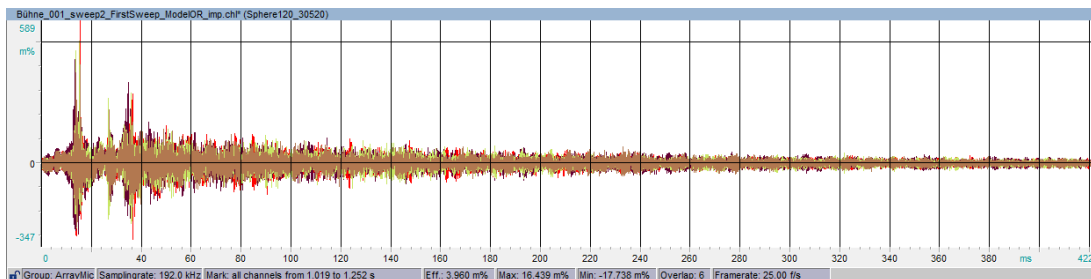


Figure 3: Time representation of the impulse response measured at the stage position.

Finally, the acoustic map delivered by the beamformer is superimposed on a 3D-model of the room under investigation to localize the direct path at the source and the early reflections on the floor, the walls, and on the ceiling of the concert hall. The first 400 ms of the impulse is presented figure [3]. Figure [4] and [5] illustrate the results of the mapping.

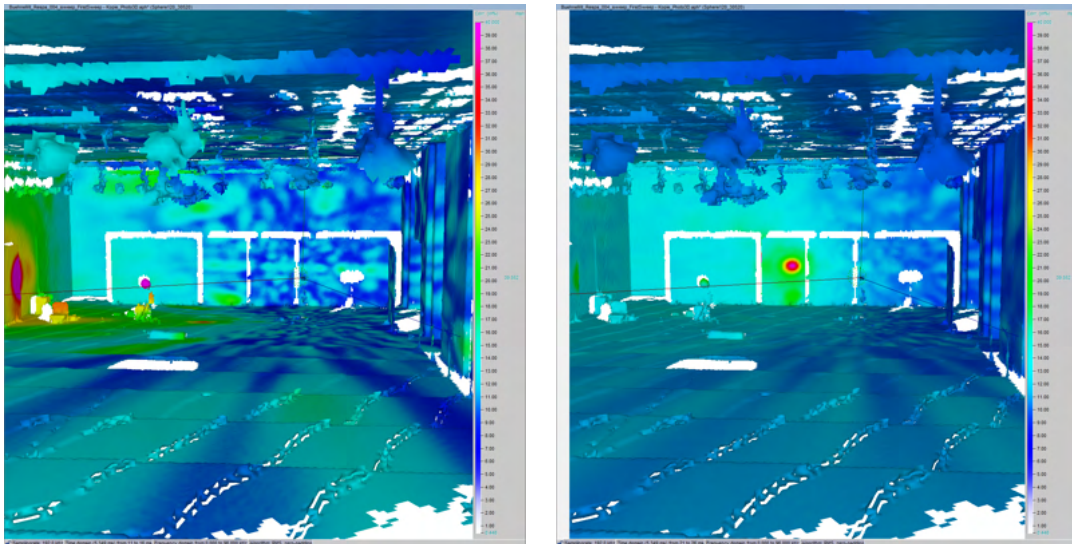


Figure 4: Mapping of the acoustic energy in the room, direct path (left) and first reflection on the standing resonator behind the stage (right).

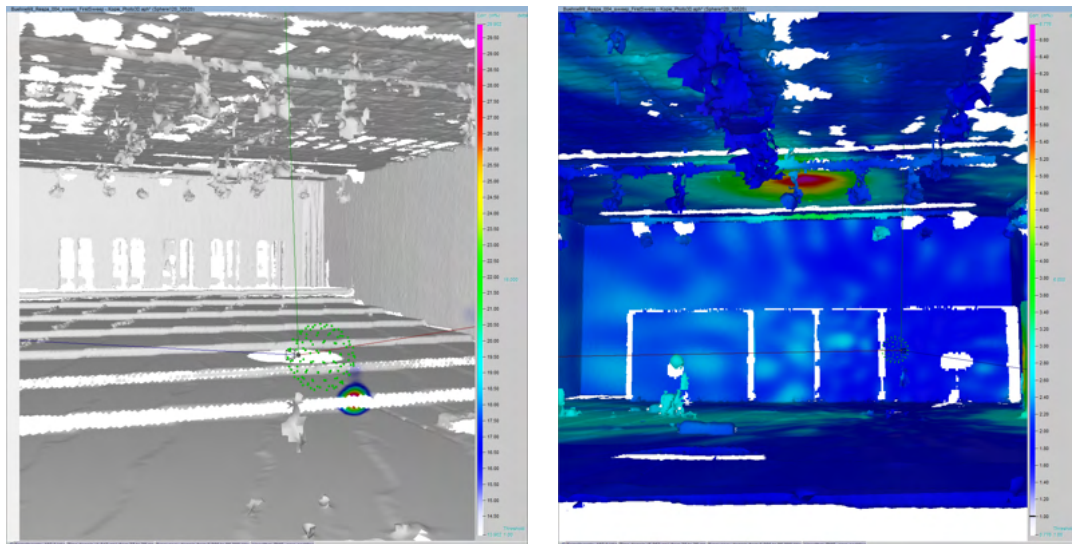


Figure 5: Mapping of the acoustic energy in the room, third reflection on the first step of the audience area, and fourth reflection on the ceiling with RESPA© panels.

4 Third octave analysis and energy decay

To analyze the reverberant field in the room more precisely, the energy decay curves in third octave bands are computed from the impulse responses. This provides us with a frequency as well as time domain decomposition of the acoustic energy in the room. Figure [6] depicts the 3rd octave frequency bands 630 Hz and 800 Hz, figure [7] the 1600 Hz and 2000 Hz frequency bands. The red curves depict the measurements performed with the acoustic treatment, the blue those without treatment.

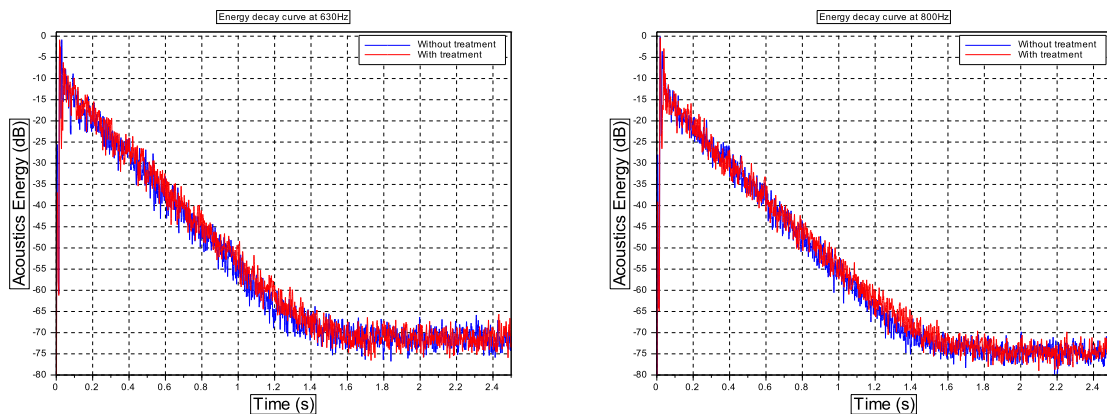


Figure 6: Energy Decay curve at the stage measurement position without and with RESPA© panels (blue and red curves respectively) left: 630 Hz , right: 800 Hz.

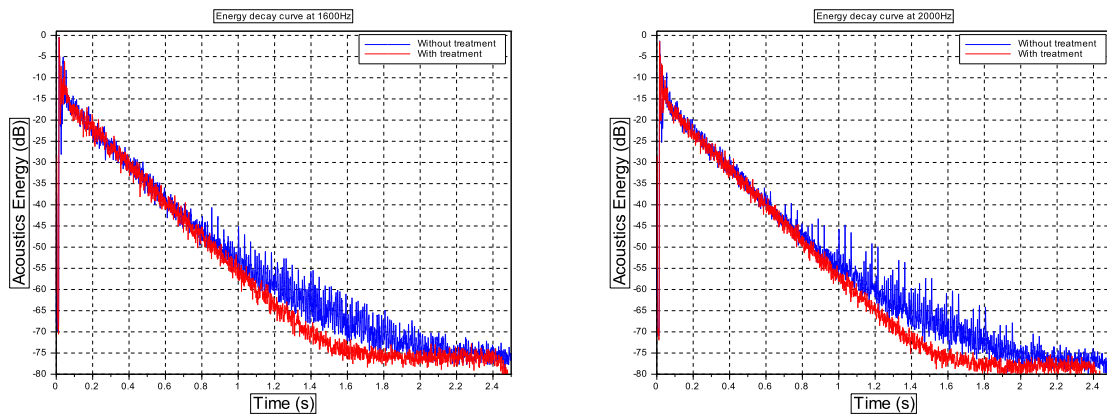


Figure 7: Energy decay curve at the stage measurement position without and with RESPA© resonator (blue and red curves respectively) left: 1600 Hz , right: 2000 Hz.

Using this type of analysis and averaging over the microphones of the array, the flutter echo is clearly visible. The corrections effected by the acoustic treatment are also well visible at the later part of the energy curve: the slope of the energy decay remains constant and homogeneous;

whereas high peaks, corresponding to the reflections, have totally disappeared. To be able to localize the reflections responsible for the flutter echo, the 3D mapping of an energy peak of the 2000 Hz third-octave band (depicted figure [8], left) is computed. The mapping of the same time interval of the measurement with the wooden panels is also depicted for comparison (right). As expected, the energy distribution in the room is much more homogeneous after the acoustic treatment. As a comparison, the pictures figure [9] present the mapping of the acoustic energy in the room without treatment. The selected time range is taken at the exact position (left) and just after a peak (right) appearing at the very beginning of the flutter echo. On the second map, the energy appears well distributed on the walls of the room. This confirms that at that time, the acoustic energy did not start to echo back and forth between the parallel walls of the hall.

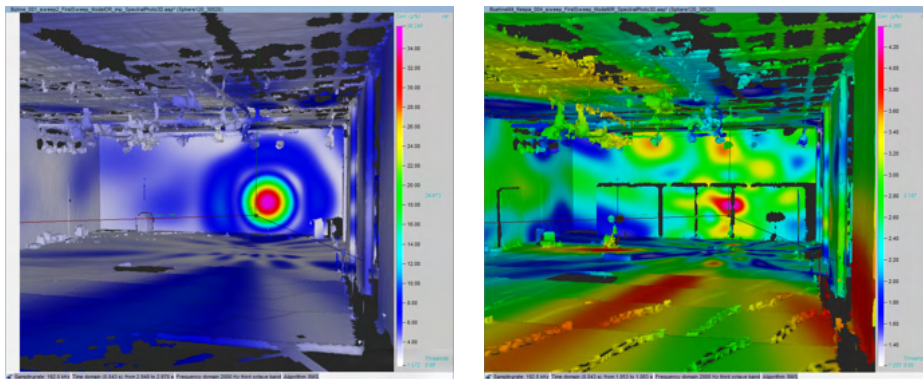


Figure 8: Mapping of the acoustic energy in the room energy peak of the 2000Hz 3rd octave band, without and with RESPA© panel.

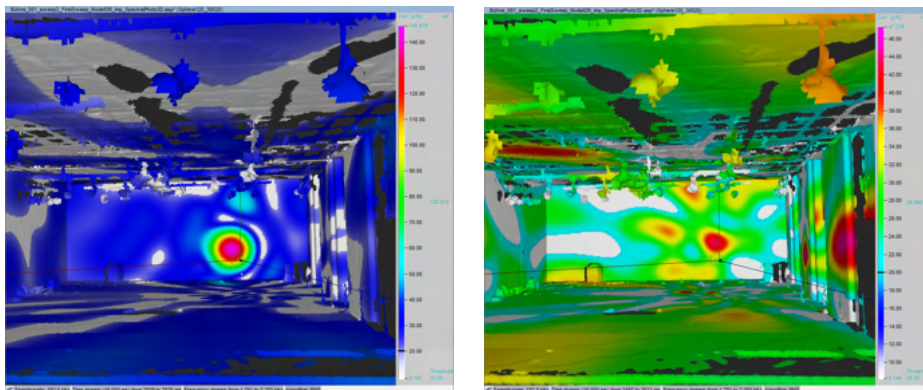


Figure 9: Mapping of the acoustic energy in the room without treatment. Selected time range at the exact position (left) and just after a peak (right) appearing at the very beginning of the flutter echo.

5 Late reverberation: spacial distribution of the acoustic energy

The spacial distribution of the acoustic energy in the room is analyzed with a mapping of the 600 ms following the early reflections (98 - 698 ms of the impulse response). The picture on the left, representing the sound field in the room without the acoustic resonators, reveals the high energy reflections between the front and back walls of the hall. In comparison, these reflections are attenuated by the treatment as shown in picture [10] on the right. This analysis can be refined using a differential acoustic photo in which the level difference at each point of two acoustic maps is computed and presented on a color scale. Figure [11] depicts the difference between of the acoustic maps at the stage position: the minuend being the map with treatment, the subtrahend the map without treatment. The color scale extends from -1.2 dB to 1.2 dB. The predominance of the reflections on the back wall of the hall and the positive effect of the treatment can be observed at the green and blue areas (the negative values): they delimit the areas at which the energy diminished between the two measurements. Inversely, the positive values (yellow-red-magenta areas) delineate the areas at which the acoustic reflections increased. Their absolute strength did not necessarily increase but with the flutter echo being eliminated, their relative strength at the measurement position increased and the sound field homogenized.

The frequency distribution of the differential energy can be determined from the result and represented graphically (figure [12]).

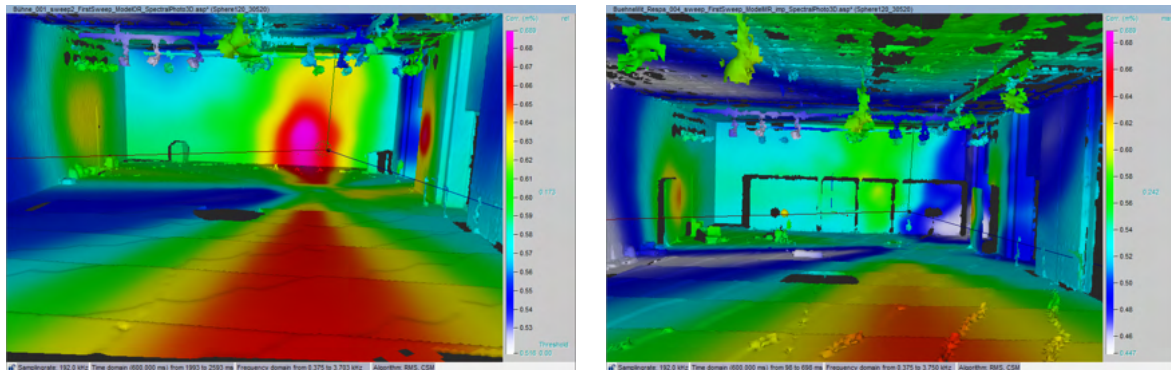


Figure 10: Mapping of the late reverberation at the stage measurement position. Left no treatment, right with treatment.

6 Room acoustics parameters

The subjective impression given by the acoustic field in the room is usually characterized with the help of acoustical parameters. Those which have acquired the widest acceptance and have been subject to standardization are the reverberation time T_{20} , the early decay time EDT , Clarity C_{80} and Definition D_{50} (ISO-3382 [2]).

The decay the sound energy undergoes after the impulse excitation is characterized by T_{20} . It is obtained by calculating the slope of the energy curve after it has been integrated starting from

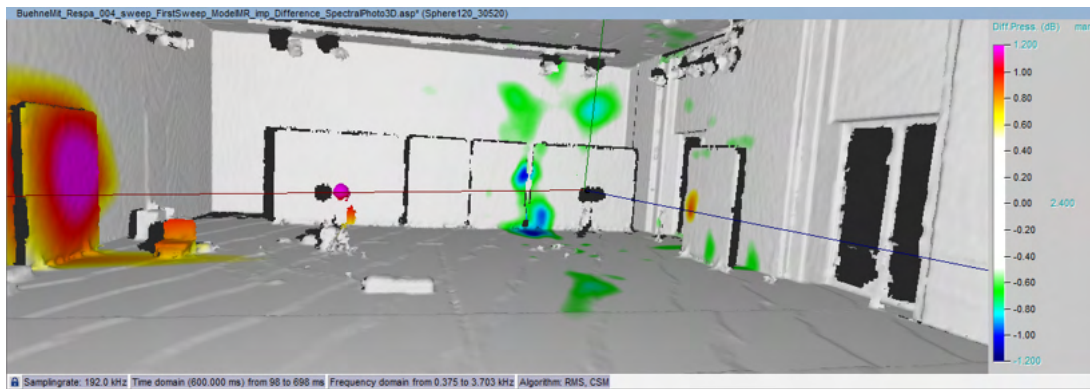


Figure 11: Difference photo of the acoustic energy (level difference at each point of two measurements).

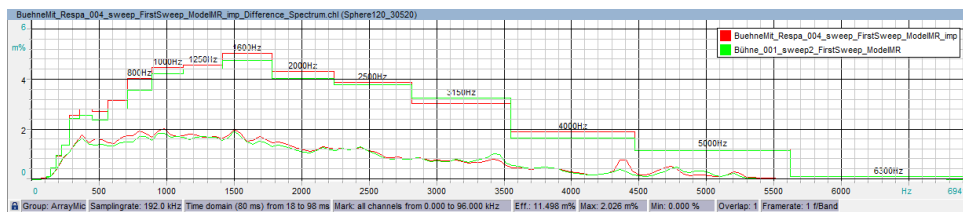


Figure 12: Frequency analysis of the difference photo.

the end (Schröder integration [6]). The EDT parameter is similar to the T_{20} with the difference that the slope is determined by the first 10 dB decays of the curve instead of 30 dB for the T_{20} . The first part of the impulse response is essential for the transmission quality of the information between the source (speaker or music instrument) and the receiver (the audience). This is what the *Clarity* and *Definition* parameters attempt to characterize (Kuttruff, [3]). Their definitions are given equation [2].

$$\begin{array}{cc}
 \textbf{Clarity:} & \textbf{Definition:} \\
 C_{80} = 10 \log \left[\frac{\int_0^{80} g(t)^2 dt}{\int_{80}^{\infty} g(t)^2 dt} \right] \text{ dB} & D_{50} = \left[\frac{\int_0^{50} g(t)^2 dt}{\int_0^{\infty} g(t)^2 dt} \right] 100\% \quad (2)
 \end{array}$$

Their computation was performed on the averaged data collected by the microphones of the array. Figure [13] presents the results thereof before (blue curves) and after the acoustic treatment (red curves) for the *Stage* and *Audience* measurement position. As expected, the parameters' overall tendency will follow the corrections brought by the acoustic treatment: the EDT and reverberation time are slightly lowered at the frequencies at which the flutter was most prominent because the energy decay becomes more homogeneous. It is to be noted that the *Definition* and *Clarity* parameters are much more sensitive to the corrections.

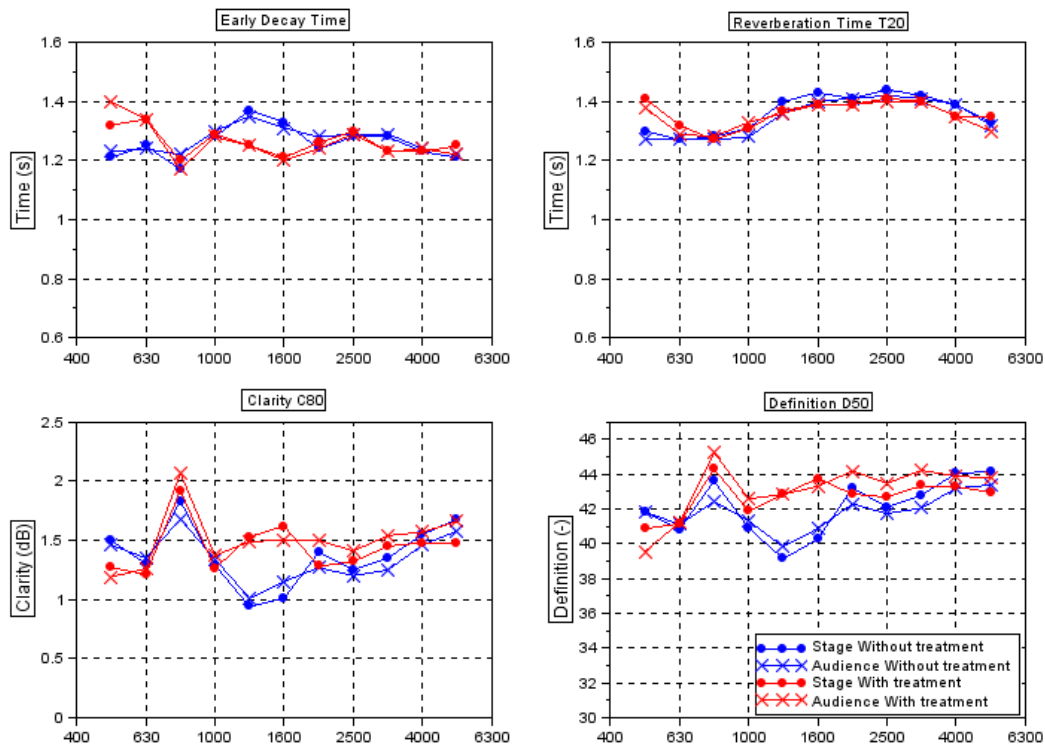


Figure 13: Room Acoustic parameters of the Werner Otto Saal, stage and audience measurement positions, before (blue curves) and after treatment (red curves).

7 Conclusion

The application of the beamforming technology with a spherical microphone array in combination with room impulse response measurements by deterministic signal can deliver a detailed insight of the sound propagation mechanisms. Confronting the results given by beamforming the conventional frequency decomposition as well as the acoustic parameters shows the coherence of the analysis. The system also includes differential acoustic map computation which offers the possibility to visualize the effects of local modifications and treatment applied to a room, and illustrate the results of an optimization. It is a very powerful tool that provides the acoustician with visualizations of the sound propagation in a room and can assist them in their work of room and building acoustic optimization.

Acknowledgment

We thank MMT Network GmbH for their very professional support of the standard room acoustic measurements. Thanks also go to our colleagues at gfai tech GmbH for their active help with the measurements and to the technical directorate of the Konzerthaus Berlin for giving us access to the measurement venue.

This research work has been funded by the German Federal Ministry for Economic Affairs and Energy (Bundesministerium für Wirtschaft und Energie, BMWi) under project registration number MF130141.

References

- [1] ISO-18233:2006. “Acoustics – application of new measurement methods in building and room acoustics.” ISO ISO-18233:2006, International Standard Organisation, Geneva, Switzerland, 2006.
- [2] ISO-3382:2008. “Acoustics – measurement of room acoustic parameters – part 2: Reverberation time in ordinary rooms.” ISO ISO-3382:2008, International Standard Organisation, Geneva, Switzerland, 2008.
- [3] H. Kuttruff. *Room Acoustics, Fourth Edition*, chapter 7 Characterisation of subjective effects, pages 190–233. Taylor & Francis, 2000. ISBN 9780419245803.
- [4] S. Müller and P. Massarani. “Transfer-function measurement with sweeps.” *Journal of the Audio Engineering Society*, 49(6), 443–471, 2001. URL <http://www.aes.org/e-lib/browse.cfm?elib=10189>.
- [5] Neugebauer, Barré, and Döbler. “Application of correlation analyses in 2d and 3d beamforming.” In *Proceedings on CD of the 5th Berlin Beamforming Conference, 19-20 February 2014*. GFaI, Gesellschaft zu Förderung angewandter Informatik e.V., Berlin, 2014. ISBN 978-3-942709-12-5. URL <http://bebec.eu/Downloads/BeBeC2014/Papers/BeBeC-2014-06.pdf>.
- [6] M. R. Schroeder. “New method of measuring reverberation time.” *The Journal of the Acoustical Society of America*, 37(3), 409–412, 1965. doi:<http://dx.doi.org/10.1121/1.1909343>. URL <http://scitation.aip.org/content/asa/journal/jasa/37/3/10.1121/1.1909343>.